THE JOURNAL OF BIOLOGICAL CHEMISTRY
Vol. 280, No. 19, Issue of May 13, pp. 18943–18949, 2005
Printed in U.S.A.

Structural Characterization of a Novel Cbl Phosphotyrosine Recognition Motif in the APS Family of Adapter Proteins*

Received for publication, December 16, 2004, and in revised form, February 17, 2005
Published, JBC Papers in Press, February 28, 2005, DOI 10.1074/jbc.M414157200

Junjie Hu and Stevan R. Hubbard‡

From the Structural Biology Program, Skirball Institute of Biomolecular Medicine and Department of Pharmacology, New York University School of Medicine, New York, New York 10016

The Cbl adapter proteins typically function to down-regulate activated protein tyrosine kinases and other signaling proteins by coupling them to the ubiquitination machinery for degradation by the proteasome. Cbl proteins bind to specific tyrosine-phosphorylated sequences in target proteins via the tyrosine kinase-binding (TKB) domain, which comprises a four-helix bundle, an EF-hand calcium-binding domain, and a non-conventional Src homology-2 domain. The previously derived consensus sequence for phosphotyrosine recognition by the Cbl TKB domain is N*X*pY(S/T)*XX*P (*X* denotes lesser residue preference), wherein specificity is conferred primarily by residues C-terminal to the phosphotyrosine. Cbl is recruited to and phosphorylated by the insulin receptor in adipose cells through the adapter protein APS. APS is phosphorylated by the insulin receptor on a C-terminal tyrosine residue, which then serves as a binding site for the Cbl TKB domain. Using x-ray crystallography, site-directed mutagenesis, and calorimetric studies, we have characterized the interaction between the Cbl TKB domain and the Cbl recruitment site in APS, which contains a sequence motif, RA(V/I)*X*NQpY(S/T), that is conserved in the related adapter proteins SH2-B and Lnk. These studies reveal a novel mode of phosphopeptide interaction with the Cbl TKB domain, in which N-terminal residues distal to the phosphotyrosine directly contact residues of the four-helix bundle of the TKB domain.

The Cbl family of adapter proteins comprises three mammalian members: c-Cbl, Cbl-b, and Cbl-c/Cbl-3. These proteins typically serve as E3 ubiquitin ligases targeting signaling proteins, such as activated protein tyrosine kinases, to the proteasome or lysosome for degradation (1). The importance of Cbl (generic for c-Cbl, Cbl-b, and Cbl-c) for down-regulating signaling pathways is underscored by the cell-transforming properties of two Cbl variants, v-Cbl (2) and 70Z-Cbl (3), in which E3 ubiquitin ligase activity is compromised.

Cbl has also been implicated as a positive regulator of intracellular signaling. For example, c-Cbl enhances mitogen-activated protein kinase activity in response to the stimulation of c-Met (4), and Cbl-b potentiates activation of phospholipase C-γ2 in B cells (5). In addition, there is evidence that Cbl plays a positive role in insulin-stimulated glucose uptake in adipose cells (6–8).

The N-terminal portion of Cbl functions as a phosphotyrosine-recognition module and consists of a four-helix bundle, an EF-hand calcium-binding domain, and a divergent Src homology-2 (SH2)[1] domain (9). These three domains are collectively termed the tyrosine kinase-binding (TKB) domain. Following the TKB domain, Cbl possesses a RING domain, which directly binds ubiquitin-conjugating enzymes (E2). In c-Cbl and Cbl-b, the RING domain is followed by a long stretch of sequence containing numerous polyproline motifs and tyrosine phosphorylation sites, with a coiled-coil dimerization domain positioned near the C terminus.

Cbl is recruited to target proteins primarily through binding of the TKB domain to tyrosine-phosphorylated sequences. Signaling proteins that have been shown to recruit Cbl by this mechanism include the epidermal growth factor (EGF) receptor (10), LET-23 (*Caenorhabditis elegans* EGF receptor ortholog) (11), macrophage colony-stimulating factor-1 receptor (12), vascular endothelial growth factor receptor (13), Src (14), Fyn (15), Zap-70 (16), Syk (17), Sprouty-2 (18, 19), and the p75 neurotrophin receptor (20).

The insulin receptor does not contain an intrinsic Cbl TKB recruitment site. In adipocytes, however, the insulin receptor recruits and phosphorylates Cbl by means of an intermediary adapter protein, APS (adapter with pleckstrin homology and Src homology-2 domains) (21). APS is a member of a family of adapter proteins that includes SH2-B and Lnk (22). Binding of the APS SH2 domain to the phosphorylated activation segment of the insulin receptor (23) facilitates phosphorylation of Tyr-618 (rat sequence numbering) near the C terminus of APS. Phosphorylated Tyr-618 (pTyr-618) then serves as a docking site for the TKB domain of Cbl (21).

Rather than targeting the insulin receptor for ubiquitin-mediated degradation, Cbl phosphorylation by the insulin receptor leads to recruitment of a Crk-C3G complex to the receptor, with subsequent activation of TC10, a Rho family GTPase (6). Although biochemical data implicating APS and Cbl in insulin-stimulated glucose uptake have been reported (6–8), other studies have not supported this conclusion (24, 25). Nevertheless, pTyr-618 in APS has clearly been established as a Cbl recruitment site (21, 22, 26).

Previous biochemical and structural studies (9, 16) have defined a consensus sequence for recognition by the Cbl TKB

* This work was supported by an American Diabetes Association research award (to S. R. H.). The costs of publication of this article were defrayed in part by the payment of page charges. This article must therefore be hereby marked "*advertisement*" in accordance with 18 U.S.C. Section 1734 solely to indicate this fact.

The atomic coordinates and structure factors (code 1YVH) have been deposited in the Protein Data Bank, Research Collaboratory for Structural Bioinformatics, Rutgers University, New Brunswick, NJ (http://www.rcsb.org/).

‡ To whom correspondence should be addressed: Skirball Institute of Biomolecular Medicine, New York University School of Medicine, New York, NY 10016. Tel.: 212-263-8938; Fax: 212-263-2150; E-mail: hubbard@saturn.med.nyu.edu.

[1] The abbreviations used are: SH2, Src homology-2; TKB, tyrosine kinase-binding; EGF, epidermal growth factor; E2, ubiquitin carrier protein; E3, ubiquitin-protein isopeptide ligase; HA, hemagglutinin; CHO-IR, Chinese hamster ovary-insulin receptor.

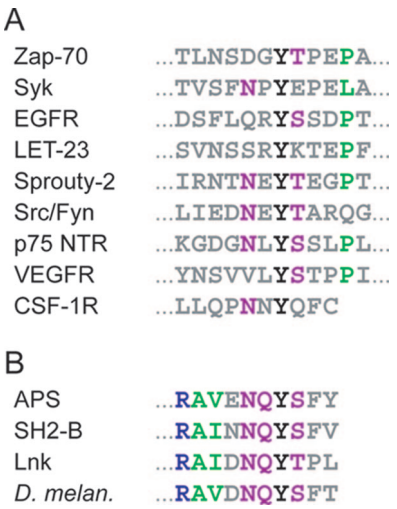

FIG. 1. **Sequence alignment of Cbl recruitment sites.** *A*, sequence alignment of previously characterized Cbl recruitment sites in a variety of signaling proteins. *Colored* (as opposed to *gray*) residues indicate those that are generally conserved. Residues colored *green* are hydrophobic, residues colored *blue* are basic, and residues colored *violet* are polar. An ellipsis (. . .) indicates that the protein sequence continues. *B*, sequences of proteins in the APS adapter family in the vicinity of the C-terminal tyrosine phosphorylation site. The sequences are for human APS, SH2-B, and Lnk, and a *Drosophila melanogaster* SH2-B ortholog (GenBank™ accession number AAF56523). Residue coloring is the same as in *A*. *EGFR*, epithelial growth factor receptor; *VEGFR*, vascular endothelial growth factor receptor; *NTR*, neurotrophin receptor; *CSF-1R*, colony-stimulating factor-1 receptor.

domain, N*X*pY(S/T)*XX*P (*X* denotes lesser residue preference). With the exception of a preference for asparagine two residues N-terminal to the phosphotyrosine (P−2), specificity for the Cbl TKB domain is thought to be conferred primarily through residues C-terminal to the phosphotyrosine, in particular, a serine or threonine at the P+1 position and a proline at the P+4 position. The Cbl recruitment sites in signaling proteins that generally match this consensus are given in Fig. 1*A*.

The sequence encompassing Tyr-618 in APS, the Cbl recruitment site near the C terminus, is conserved in SH2-B and Lnk (Fig. 1*B*). This sequence motif, RA(V/I)*X*NQpY(S/T), is striking in that the conservation extends back to arginine at the P−6 position. Moreover, the C terminus of APS (and of SH2-B and Lnk) is only three residues from the phosphotyrosine, and therefore this non-canonical Cbl recruitment site ends at the P+3 residue. To understand the molecular basis for Cbl recruitment to APS, and thus to the insulin receptor, we have determined the crystal structure of the c-Cbl TKB domain in complex with a phosphopeptide representing the Cbl recruitment site in APS. The structure shows that conserved residues N-terminal to pTyr-618, which make specific contacts with residues in the four-helix bundle of the TKB domain, play a critical role in recruitment of Cbl to APS. Accompanying site-directed mutagenesis studies of APS and c-Cbl corroborate the structural findings.

EXPERIMENTAL PROCEDURES

Production of the c-Cbl TKB Domain—The c-Cbl TKB domain was subcloned from full-length human c-Cbl into the expression vector pGEX-4T-1 (Amersham Biosciences), which includes a thrombin-cleavable N-terminal glutathione *S*-transferase tag. The construct was transformed into *Escherichia coli* strain BL21(DE3) for protein expression. The glutathione *S*-transferase fusion protein was isolated from cleared cell lysates by GSTrap (Amersham Biosciences) affinity chromatography, cleaved by thrombin to remove glutathione *S*-transferase, and further purified by Source-S (Amersham Biosciences) ion exchange chromatography. The purified protein includes residues 25–351 of human c-Cbl plus two N-terminal residues (GS) remaining from cleavage of the thrombin site. The composition of the purified protein was verified by matrix-assisted laser desorption ionization mass spectrometry. The protein was concentrated to 5 mg/ml in a centrifuge concentrator (Amicon Ultra, Millipore).

Phosphopeptides—13-Residue phosphopeptides representing the rat APS pTyr-618 phosphorylation site, GRARAVENQpYSFY, and the human EGF receptor pTyr-1045 phosphorylation site, EDSFLQRpYSSDPT, were synthesized (GeneMed Synthesis), and their masses were verified by matrix-assisted laser desorption ionization-time-of-flight mass spectrometry. The lyophilized peptides were solubilized in 50 mM Hepes, pH 8.0, and 100 mM NaCl.

X-ray Crystallography—The purified c-Cbl TKB domain and the APS pTyr-618 phosphopeptide were mixed at a 1:1.6 molar ratio. Crystals of the TKB domain-APS phosphopeptide complex were grown in hanging drops at 22 °C by mixing 2 μl of the TKB domain-phosphopeptide stock solution with 2 μl of reservoir buffer containing 18% polyethylene glycol 8000, 0.2 M magnesium or calcium acetate and 0.1 M sodium cacodylate, pH 6.1. The crystals belong to space group P6 with unit cell dimensions $a = b = 122.26$ Å, $c = 55.13$ Å for the magnesium acetate crystals, and $a = b = 121.62$ Å, $c = 54.93$ Å for the calcium acetate crystals. There is one TKB-APS complex in the asymmetric unit, giving a solvent content of 61%. Data were collected on beamline X4A at the National Synchrotron Light Source, Brookhaven National Laboratory, and were processed using Denzo/Scalepack software (27). A molecular replacement solution was found with AMoRe software (28) using the structure of the TKB domain-ZAP-70 phosphopeptide complex (9) (2CBL) as a search model. Rigid body refinement and positional and B-factor refinement were performed with Crystallography and NMR System (29), and model building was performed with O software (30). For the structure determined from crystals grown in magnesium acetate, a Mg^{2+} ion has been modeled in the Ca^{2+}-binding site of the EF-hand domain, based on the observed distances to oxygen ligands and B-factor considerations.

Site-directed Mutagenesis, Mammalian Cell Transfection, Immunoprecipitation and Immunoblotting—Antibodies to Myc (9E10) and hemagglutinin (HA) (F-7) were purchased from Santa Cruz Biotechnology. The Myc-tagged rat APS (pRK5-Myc-APS) construct and the HA-tagged human c-Cbl (pKH3-c-Cbl) construct were kindly provided by Dr. A. Saltiel. Point mutations in APS and c-Cbl were generated using the QuikChange system (Stratagene). All mutations were verified by automated DNA sequencing.

Chinese hamster ovary-IR (CHO-IR) cells were maintained in α-minimal essential medium containing 10% fetal bovine serum plus antibiotics. The cells were transfected by Lipofectamine 2000 reagent (Invitrogen). After 6 h, the medium was changed back to the above. After ~24 h, the cells were serum-deprived for 3 h in Ham's F-12 medium. Sodium orthovanadate (50 μM) was added (or not) to the cell medium 30 min prior to insulin stimulation. Cells in 60-mm-diameter dishes were treated with or without 100 nM insulin and with or without 50 μM sodium orthovanadate for 5 min, washed twice with ice-cold phosphate-buffered saline, and lysed for 30 min at 4 °C with buffer containing 50 mM Tris-HCl, pH 8.0, 135 mM NaCl, 1% Triton X-100, 1.0 mM EDTA, 1.0 mM sodium pyrophosphate, 1.0 mM sodium orthovanadate, 10 mM NaF, and protease inhibitors (Roche Diagnostics). The clarified lysates were incubated with antibodies to Myc for 1 h at 4 °C. The immune complexes were precipitated with protein A/G-agarose (Santa Cruz Biotechnology) for 1 h at 4 °C and were washed extensively with lysis buffer before solubilization in SDS-PAGE sample buffer. Bound proteins were resolved by SDS-PAGE and transferred to Immobilon-P (Millipore) polyvinylidene difluoride membranes. Individual proteins were detected with specific antibodies and visualized by blotting with horseradish peroxidase-conjugated secondary antibodies (BioSource International).

Isothermal Titration Calorimetry—The purified c-Cbl TKB domain was dialyzed overnight in a buffer containing 50 mM Hepes, pH 8.0, and 100 mM NaCl. The APS pTyr-618 phosphopeptide and the EGF receptor pTyr-1045 phosphopeptide were dissolved in the same buffer. Protein concentration was determined by UV light absorption at 280 nm, and peptide concentrations were determined gravimetrically and confirmed by UV light absorption at 280 nm. Calorimetric measurements were conducted at 25 °C with a VP-ITC calorimeter (MicroCal). Each titration experiment consisted of 29 10-μl injections (5 μl for the first injection) of phosphopeptide into the calorimetric cell containing 1.34 ml of the protein solution, with a 5-min interval between each injection. Titration data were processed using ORIGIN software (MicroCal). A small heat of dilution, calculated from the last several injections, was subtracted prior to curve fitting. The thermal constants were derived using a one-site binding model for fitting, varying N (binding stoichiometry), K_D (dissociation constant) and ΔH (reaction enthalpy) (31). From these values, the free energy (ΔG) and entropy change (ΔS) upon

TABLE I
X-ray data collection and refinement statistics

Data collection	
Resolution (Å)	50.0–2.05
Observations (>1σ)	163,581
Unique reflections	29,857
Completeness (%)	100.0 (100.0)[e]
Redundancy	5.5 (4.5)[e]
R_{sym}[a] (%)	6.1 (25.4)[e]
Refinement[b]	
Resolution (Å)	30.0–2.05
Reflections	29,028
R_{cryst}[c]/R_{free} (%)	20.9/24.7
Root-mean-square deviations	
Bond lengths (Å)	0.006
Bond angles (°)	1.2
B-factors[d] (Å^2) (main chain/side chain)	0.8/1.2
Average B-factors (Å^2)	
TKB domain	30.3
APS phosphopeptide	31.0
Water	34.5
Mg^{2+} ion	27.1

[a] $R_{sym} = 100 \times \Sigma |I - \langle I \rangle| / \Sigma I$.
[b] Atomic model includes 2488 TKB domain atoms, 82 phosphopeptide atoms, 1 Mg^{2+} ion and 188 water molecules.
[c] $R_{cryst} = 100 \times \Sigma ||F_o| - |F_c|| / \Sigma |F_o|$, where F_o and F_c are the observed and calculated structure factors, respectively ($F_o > 0\sigma$). R_{free} determined from 5% of the data.
[d] For bonded atoms.
[e] Value in parentheses is for the highest resolution shell (2.12–2.05 Å).

peptide binding can be calculated using the equation $-RT\ln(1/K_D) = \Delta G = \Delta H - T\Delta S$, where R is the universal molar gas constant, and T is the absolute temperature. The c values (K_A·[TKB domain]) for the calorimetry experiments were 253 (APS phosphopeptide) and 32 (EGF receptor phosphopeptide).

RESULTS

Crystal Structure of the c-Cbl TKB Domain in Complex with the APS pTyr-618 Phosphopeptide—Crystals of the complex between the c-Cbl TKB domain and the APS-derived phosphopeptide (TKB-APS) were obtained in conditions similar to those described for the crystals of the TKB domain complexed with a Zap-70-derived phosphopeptide (TKB-Zap-70) (9), with either Ca^{2+} or Mg^{2+} as the divalent cation. Crystal structures of both the Ca^{2+} and Mg^{2+} forms were determined by molecular replacement, using the structure of TKB-Zap-70 (9) as a search model. The structures have been refined at 2.3 Å (Ca^{2+}) and 2.05 Å (Mg^{2+}) resolution. The two structures are virtually identical, and therefore the higher resolution Mg^{2+} structure was used in the structure analysis that follows. Data collection and refinement statistics for the Mg^{2+} structure are given in Table I, and an electron density map in the vicinity of the APS phosphopeptide is shown in Fig. 2.

Overall, the crystal structure of TKB-APS (Fig. 3*A*) is very similar to that of TKB-Zap-70 (9), with a root mean square deviation of C-α positions in the TKB domain (residues 50–350) of only 0.30 Å. As in the TKB-Zap-70 structure, the four-helix bundle, EF-hand domain and SH2 domain make extensive interdomain contacts. The striking difference between the two structures is the differential interactions of the two phosphopeptides with the SH2 domain and four-helix bundle of the TKB domain (Fig. 3*B*).

In the TKB-Zap-70 structure, the interaction between the phosphopeptide and the TKB domain is mediated primarily by the phosphotyrosine and residues C-terminal to the phosphotyrosine, which interact with residues in the SH2 domain (Fig. 3*B*). Residues N-terminal to the phosphotyrosine, beyond P−2, are disordered in the TKB-Zap-70 structure. In contrast, in the TKB-APS structure, the interaction is mediated primarily by the phosphotyrosine and residues N-terminal to the phosphotyrosine, which are well ordered in the structure back to

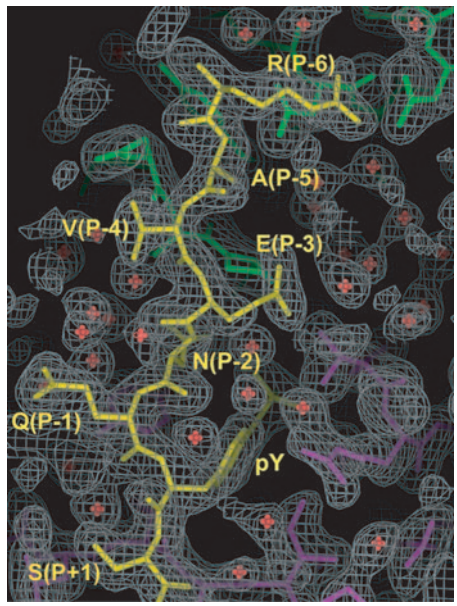

FIG. 2. **Electron density map in the phosphopeptide-binding site of the c-Cbl TKB domain.** The $2F_o - F_c$ electron density map (2.05-Å resolution, 1σ contour) is shown as *wire mesh* (*gray*) with the refined atomic model superimposed. Residues of the APS phosphopeptide are *yellow*, residues of the four-helix bundle are *green*, and residues of the SH2 domain are *purple*. Ordered water molecules are indicated with *red crosses*. Residues of the APS phosphopeptide are labeled. The figure was prepared using PYMOL software (www.pymol.org).

Arg(P−6) (Fig. 2), the beginning of the conserved sequence motif.

Several of the APS N-terminal residues make direct contacts with residues of the four-helix bundle (Fig. 3*B*). Arg(P−6) is salt-bridged to Asp-90 (Fig. 3*C*), which extends from α-helix B (αB) in the four-helix bundle. The Ala(P−5) side chain lies in a shallow hydrophobic slot formed by residues in the αA-αB linker of the four-helix bundle. Both Arg(P−6) and Ala(P−5) are strictly conserved in the APS adapter family. Val(P−4) points away from the surface of the four-helix bundle and is solvent-exposed. The side chain of Glu(P−3), which is poorly ordered, is also devoid of TKB domain contacts. The Gln(P−1) side chain is well ordered in the structure, but this is because of a hydrogen-bonding interaction with a symmetry-related molecule.

The side chain of Asn(P−2) makes several interactions that explain its conservation, not only in the APS pTyr618 motif, but also in the previously recognized consensus sequence for binding of the TKB domain (Fig. 1*A*). The amide nitrogen of the Asn(P−2) side chain is hydrogen-bonded to the phosphate group of phosphotyrosine and to the carbonyl oxygen of Pro-81 (αA-αB linker) of the four-helix bundle (Fig. 3*C*). The amide oxygen of the Asn(P−2) side chain makes a water-mediated hydrogen bond with the Asp-275 side chain (αA) of the SH2 domain. These structural observations are consistent with the strong preference for asparagine at the P−2 position, as determined from a degenerate peptide library study (16). In the TKB-Zap-70 structure, the side chain of Asp(P−2) was poorly ordered but positioned similarly to Asn(P−2) in the TKB-APS structure.

In addition to side-chain interactions, residues of the four-helix bundle are hydrogen-bonded to backbone atoms of the phosphopeptide (Fig. 3*C*). Asn-79 (αA-αB linker) is hydrogen-bonded to the carbonyl oxygen of Arg(P−6), and Asp-86 (αB) is hydrogen-bonded to the backbone nitrogen of Ala(P−5). A backbone-backbone hydrogen bond is observed between Asn-79 and Val(P−4). As in the TKB-Zap-70 structure, Tyr-274 (αA) in

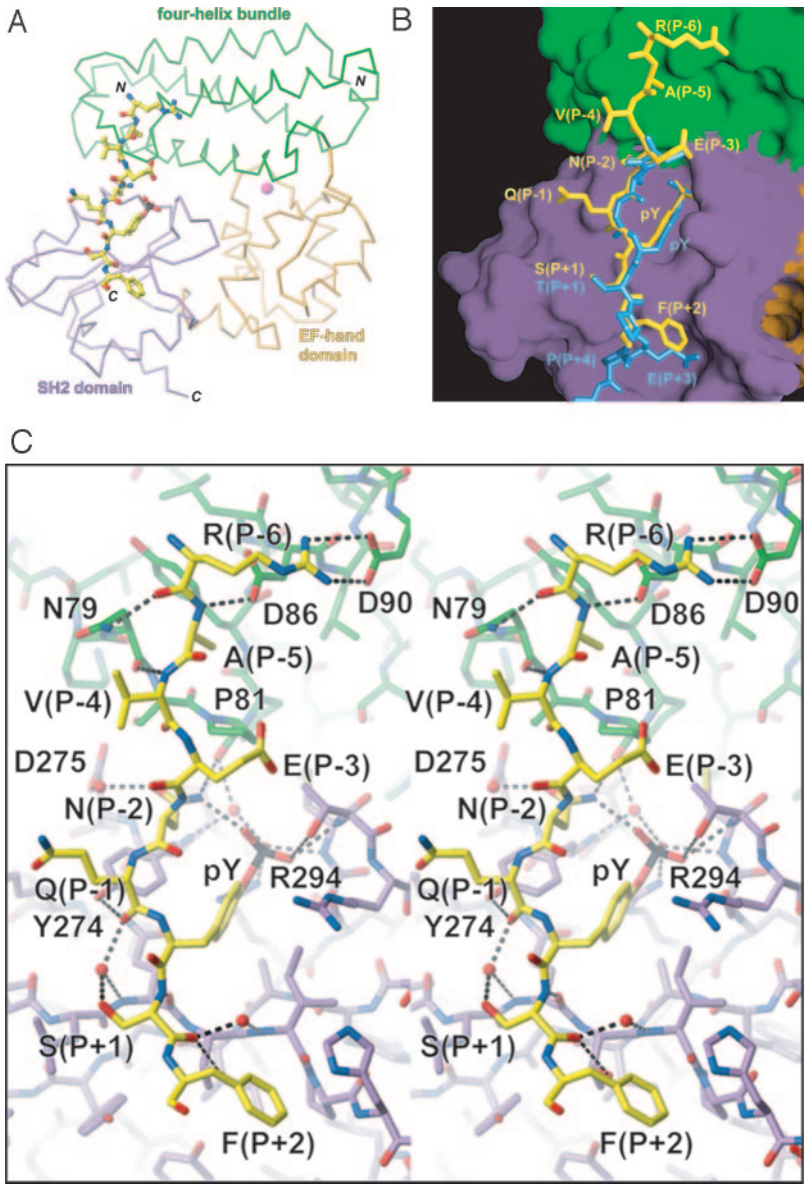

FIG. 3. **Crystal structure of the c-Cbl TKB domain in complex with the APS pTyr-618 phosphopeptide.** *A*, C-α trace of the c-Cbl TKB domain with the bound APS phosphopeptide shown in *ball-and-stick* representation. The four-helix bundle of the TKB domain is colored *green*, the EF-hand domain is colored *orange*, and the SH2 domain is colored *purple*. Carbon atoms of the APS phosphopeptide are colored *yellow*, oxygen atoms, *red*, and nitrogen atoms, *blue*. The Mg^{2+} ion in the EF-hand domain is represented by a *magenta sphere*. The N and C termini of the phosphopeptide and the TKB domain are indicated (*N* and *C*). *B*, molecular surface representation of the TKB domain. The surfaces of the four-helix bundle, the EF-hand domain, and the SH2 domain are colored as in *A*. The APS phosphopeptide is colored *yellow*, and the superimposed Zap-70 phosphopeptide from the TKB-Zap-70 crystal structure (9) is colored *cyan*. *C*, stereo view showing the interactions between the APS phosphopeptide and the c-Cbl TKB domain. Carbon atoms are colored according to domain, as in *A*. Oxygen atoms are colored *red*, nitrogen atoms, *blue*, and sulfur atoms (in the TKB domain), *yellow*. Water molecules are represented by *red spheres*. Hydrogen bonds/salt bridges are represented by *black dashed lines*. The figure was prepared using MOLMOL (*A* and *C*) (36) and GRASP (*B*) (37) software.

the SH2 domain is hydrogen-bonded to the carbonyl oxygen of the P−1 residue.

The phosphate group of the phosphotyrosine is bound in the canonical phosphate-binding pocket of the SH2 domain, salt-bridged to SH2-invariant Arg-294 (βB) (Fig. 3*C*). Residues in the BC loop of the c-Cbl SH2 domain also provide phosphate coordination through backbone and side-chain interactions, very similar to that observed in the crystal structures of the Lck and Src SH2 domains bound to high affinity phosphopeptides (32, 33). As in the TKB-Zap-70 structure, one water-mediated hydrogen bond is made between the phosphate group and the carbonyl oxygen of Pro-81 (αA-αB linker) of the four-helix bundle.

In contrast to the TKB-Zap-70 structure, the only well ordered residue C-terminal to the phosphotyrosine in the TKB-APS structure is Ser(P+1), which makes water-mediated hydrogen bonds with the backbone nitrogen of Gln-316 (βD, SH2 domain) and the carbonyl oxygen of Gln(P−1). These interactions are also observed in the TKB-Zap-70 structure for Thr(P+1). Serine or threonine is reasonably well conserved at the P+1 position (Fig. 1). Phe(P+2) is included in the atomic model but is poorly ordered, whereas Tyr(P+3), the C-terminal residue of the phosphopeptide (and of APS itself) is disordered.

Site-directed Mutagenesis of APS and c-Cbl—To verify that the interactions observed in the crystal structure between the APS pTyr-618 phosphopeptide and the c-Cbl TKB domain are important for Cbl recruitment to APS in cells, mutations were introduced in the conserved sequence motif encompassing Tyr-618 in full-length APS. Myc-tagged wild-type or mutant APS was transiently transfected into CHO-IR cells together with HA-tagged c-Cbl, and co-immunoprecipitation experiments were performed.

For several of the APS mutants, we observed differences in insulin-stimulated phosphorylation levels *versus* wild-type APS (data not shown), which are evidently due to sequence changes that affect phosphorylation of Tyr-618 by the insulin receptor or dephosphorylation of pTyr-618 by tyrosine phosphatases, or both. For the purpose of examining c-Cbl recruitment to the APS mutants, the phosphatase inhibitor vanadate was included in the cell medium prior to and during insulin stimulation to obtain approximately equal phosphorylation levels for wild-type and mutant APS proteins (Fig. 4*A*, *third blot* from *top*).

The results of co-immunoprecipitation of c-Cbl with the various APS mutants are shown in Fig. 4*A* (*top blot*). A significant loss of binding (near Y618F control levels) was observed for the

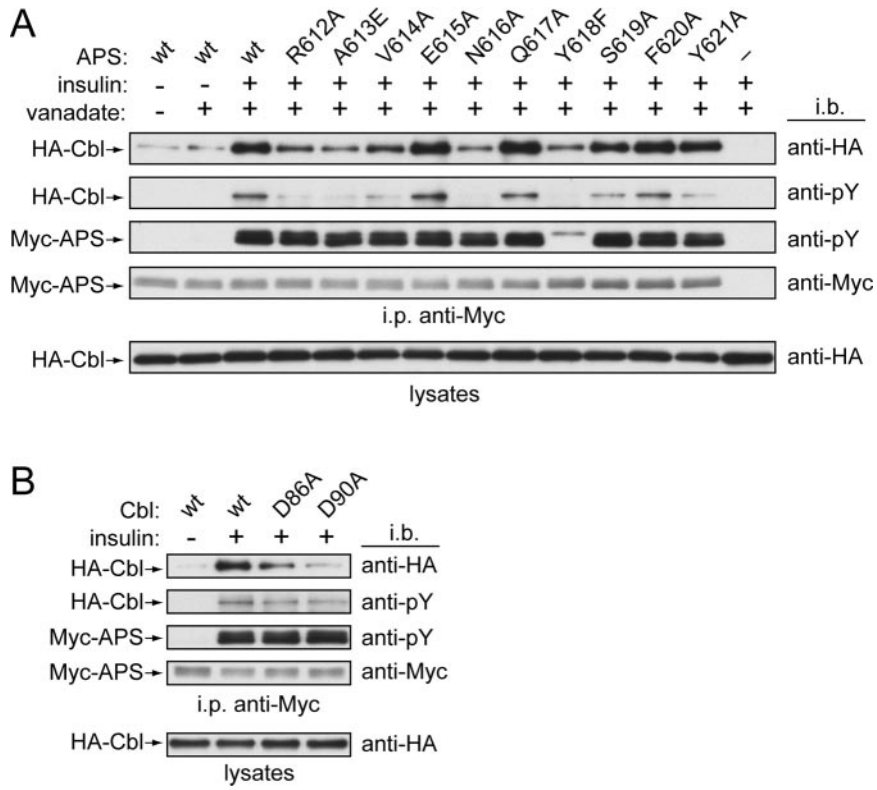

FIG. 4. **Site-directed mutagenesis of APS and c-Cbl.** *A*, Myc-tagged APS (wild-type (*wt*) or mutant) and HA-tagged c-Cbl were co-transfected into CHO-IR cells. After treatment with or without insulin and in the presence or absence of sodium orthovanadate, cells were lysed and immunoprecipitated with an anti-Myc antibody. Immunoprecipitates (*i.p.*) were immunoblotted (*i.b.*) using antibodies to HA (*top blot*), to phosphotyrosine (*second* and *third blots*), or to Myc (*fourth blot*). The lysates were analyzed by Western blotting using an anti-HA antibody to show approximately equal amounts of HA-Cbl (*bottom*). *B*, wild-type Myc-APS and wild-type or mutant (in the four-helix bundle) HA-Cbl were co-transfected into CHO-IR cells. Co-immunoprecipitation and immunoblotting are the same as in *A*, with sodium orthovanadate present prior to and during insulin stimulation. The identification of the bands appears on the *left side* of all blots.

APS N-terminal mutations R612A (P−6), A613E (P−5) and N616A (P−2), which is consistent with the structural observations (Fig. 3*C*). V614A (P−4) also resulted in a loss of c-Cbl binding, although in the crystal structure, the valine side chain makes no contacts with the TKB domain. It is conceivable that valine or isoleucine is conserved at this position to favor binding by influencing the local backbone conformation. Both of these Cβ-branched residues have a high propensity for adopting an extended (β) backbone conformation (34), the conformation observed in the crystal structure. Alanine substitutions at Glu-615 (P−3) and Gln-617 (P−1) did not affect the amount of c-Cbl co-immunoprecipitated, consistent with the lack of interaction of these two residues with c-Cbl in the TKB-APS structure. Curiously, glutamine is conserved at the P−1 position in the APS adapter family across all species. On the C-terminal side of Tyr-618, the APS mutants co-immunoprecipitated similar amounts of c-Cbl as wild-type APS (Fig. 4*A*, *top blot*). Phosphorylation of c-Cbl by the insulin receptor (Fig. 4*A*, *second blot from top*) correlated well with the amount of c-Cbl co-immunoprecipitated with the APS mutants.

To provide evidence that Asp-86 and Asp-90 in the c-Cbl four-helix bundle interact with residues N-terminal to pTyr-618, as observed in the crystal structure (Fig. 3*C*), these aspartic acid residues in c-Cbl were mutated to alanine. As judged by co-immunoprecipitation, these four-helix bundle residues, particularly Asp-90, which forms a salt bridge with Arg-612 (P−6), are important for binding to APS (Fig. 4*B*, *top blot*). Of note, all of the residues of the four-helix bundle that interact with the APS phosphopeptide, Asn-79, Asp-86, and Asp-90, are conserved in the three mammalian Cbl proteins.

Measurement of TKB Domain-Phosphopeptide Binding Affinity—To determine the affinity of the interaction between the APS pTyr-618 site and the TKB domain of c-Cbl, isothermal titration calorimetry experiments were performed. The dissociation constant (K_D) for binding of the APS phosphopeptide to the c-Cbl TKB domain was determined to be 43 nM (Fig. 5*A*). To compare this affinity with that of a conventional Cbl recruitment site, the K_D for an EGF receptor phosphopeptide representing the pTyr-1045 site (Fig. 1*A*) was also measured. This site, which is similar to the Cbl recruitment site in Zap-70, contains favored residues at the P+1 (serine) and P+4 (proline) positions but lacks asparagine at the P−2 position. The measured K_D for the interaction between the EGF receptor phosphopeptide and the TKB domain was 348 nM (Fig. 5*B*) or ~8-fold higher (*i.e.* lower affinity) than the K_D for the APS phosphopeptide.

DISCUSSION

Numerous signaling proteins have been shown to recruit Cbl in a phosphorylation-dependent manner. The conventional tyrosine phosphorylation sites to which Cbl is recruited show moderate sequence conservation (Fig. 1*A*). Asparagine is present at the P−2 position (relative to phosphotyrosine) more often than not, as is serine/threonine at the P+1 position and proline at the P+4 position (N*X*pY(S/T)*XX*P). The structural basis for these preferences has been elucidated in the previous TKB-Zap-70 structure (P+1, P+4) (9) and in the present study (P−2, P+1). Interestingly, of the conventional Cbl recruitment sites, only those in Sprouty-2 and the p75 neurotrophin receptor contain preferred residues at all three positions (Fig. 1*A*).

A novel Cbl recruitment site was recently identified in the juxtamembrane region of c-Met (35). Along with phosphotyrosine, an aspartic acid at the P−1 position and an arginine at the P+1 position (DpYR) are the critical residues for Cbl binding. The mode of binding of this phosphorylated sequence to the Cbl TKB domain has not been elucidated, and it is unclear why this motif would exhibit specificity for the Cbl TKB domain *versus* other SH2 domains.

The sequence surrounding the Cbl recruitment site near the C terminus of the adapter protein APS is highly conserved in SH2-B and Lnk (Fig. 1*B*), the other members of this adapter family. Compared with conventional Cbl recruitment sites, the conservation in the APS Tyr-618 motif extends from arginine at the P−6 position to a serine or threonine at P+1, RA(V/I)*X*N-

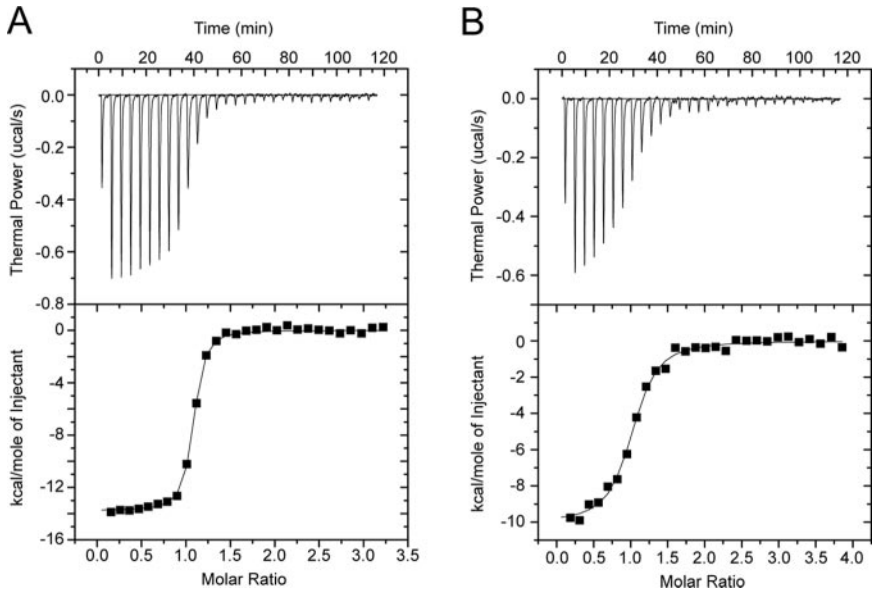

FIG. 5. **Measurement of binding affinities.** The binding affinities of the APS pTyr-618 (*A*) and the EGF receptor pTyr-1045 (*B*) phosphopeptides to the c-Cbl TKB domain were measured using isothermal titration calorimetry. The concentration of the TKB domain was 11 μM in both experiments. The concentration of the APS phosphopeptide was 167 μM, and the concentration of the EGF receptor phosphopeptide was 200 μM. The *top panels* in both *A* and *B* show the injection profile after baseline correction, and the *bottom panels* show the integration (heat release) for each injection (except the first one). The *solid lines* in the *bottom panel* show the fit of the data to a function based on a one-site binding model. For binding of the APS phosphopeptide to the TKB domain, the observed binding constant K_A is $2.35 \pm 0.22 \times 10^7$ M^{-1} (K_D = 43 nM), with a stoichiometry, N, of 1.04 ± 0.01, an enthalpic contribution to binding, ΔH, equal to -13.78 ± 0.07 kcal/mol, and an entropic contribution, $T\Delta S$, equal to -3.71 kcal/mol, for a free energy change, ΔG, of -10.07 kcal/mol. For binding of the EGF receptor phosphopeptide to the TKB domain, $K_A = 2.87 \pm 0.38 \times 10^6$ M^{-1} (K_D = 348 nM), $n = 0.99 \pm 0.01$, $\Delta H = -10.05 \pm 0.17$ kcal/mol, $T\Delta S = -1.23$ kcal/mol and $\Delta G = -8.82$ kcal/mol.

QpY(S/T). Of note, the C terminus of these adapter molecules is just three residues beyond the phosphorylation site, *i.e.* there is no P+4 residue. This is also true for the Cbl-binding site at the C terminus of the colony-stimulating factor-1 receptor (Fig. 1*A*).

The TKB-APS crystal structure reveals that residues N-terminal to pTyr-618 in APS, Arg-612 (P−6), Ala-613 (P−5), and Asn-616 (P−2) make specific contacts with residues in the four-helix bundle of the Cbl TKB domain (Fig. 3*C*). Site-directed mutagenesis of these residues confirms their importance in Cbl recruitment to APS (Fig. 4*A*). Evidence that this is a productive mode of binding comes from the measured dissociation constant for the c-Cbl TKB domain and the APS pTyr-618 site, 43 nM (Fig. 5*A*), which is approximately eight times lower than that for the EGF receptor pTyr-1045 site, a conventional Cbl recruitment site (Fig. 1*A*). It is likely that the affinities of the various Cbl recruitment sites have been fine-tuned, through sequence variation, to provide the appropriate strength of Cbl engagement for a particular signaling output, either positive or negative.

A pattern search of the Swiss Protein Data Base with RAΦXNQY(S/T) (Φ denotes a hydrophobic residue) yields APS, SH2-B, Lnk, and the receptor for complement component C1q (CD93). In CD93, the sequence RAMENQYSPTP is found near the C terminus of the molecule, indicating that it is likely to be accessible for phosphorylation. Assuming that this site is phosphorylated, the results of the present study suggest that CD93 is likely to be a Cbl-binding protein.

In summary, using x-ray crystallography, site-directed mutagenesis, and calorimetry, we have characterized the interaction between the c-Cbl TKB domain and a phosphopeptide representing the APS C-terminal phosphorylation site, which upon phosphorylation by the insulin receptor, becomes a recruitment site for Cbl. The results demonstrate that, in addition to the SH2 domain, the four-helix bundle of the Cbl TKB domain can make important contributions to phosphotyrosine sequence recognition and binding affinity by engaging residues N-terminal to the phosphotyrosine.

Acknowledgments—We thank Drs. A. Saltiel and J. Liu for providing reagents and for helpful discussions, and Dr. M. Mohammadi for critical reading of the manuscript.

REFERENCES

1. Sanjay, A., Horne, W. C., and Baron, R. (2001) *Sci. STKE 2001*, PE40
2. Langdon, W. Y., Hartley, J. W., Klinken, S. P., Ruscetti, S. K., and Morse, H. C. (1989) *Proc. Natl. Acad. Sci. U. S. A.* **86,** 1168–1172
3. Andoniou, C. E., Thien, C. B., and Langdon, W. Y. (1994) *EMBO J.* **13,** 4515–4523
4. Garcia-Guzman, M., Larsen, E., and Vuori, K. (2000) *Oncogene* **19,** 4058–4065
5. Yasuda, T., Tezuka, T., Maeda, A., Inazu, T., Yamanashi, Y., Gu, H., Kurosaki, T., and Yamamoto, T. (2002) *J. Exp. Med.* **196,** 51–63
6. Chiang, S. H., Baumann, C. A., Kanzaki, M., Thurmond, D. C., Watson, R. T., Neudauer, C. L., Macara, I. G., Pessin, J. E., and Saltiel, A. R. (2001) *Nature* **410,** 944–948
7. Ahn, M. Y., Katsanakis, K. D., Bheda, F., and Pillay, T. S. (2004) *J. Biol. Chem.* **279,** 21526–21532
8. Standaert, M. L., Sajan, M. P., Miura, A., Bandyopadhyay, G., and Farese, R. V. (2004) *Biochemistry* **43,** 15494–15502
9. Meng, W., Sawasdikosol, S., Burakoff, S. J., and Eck, M. J. (1999) *Nature* **398,** 84–90
10. Levkowitz, G., Waterman, H., Ettenberg, S. A., Katz, M., Tsygankov, A. Y., Alroy, I., Lavi, S., Iwai, K., Reiss, Y., Ciechanover, A., Lipkowitz, S., and Yarden, Y. (1999) *Mol. Cell* **4,** 1029–1040
11. Yoon, C. H., Chang, C., Hopper, N. A., Lesa, G. M., and Sternberg, P. W. (2000) *Mol. Biol. Cell* **11,** 4019–4031
12. Wilhelmsen, K., Burkhalter, S., and van der Geer, P. (2002) *Oncogene* **21,** 1079–1089
13. Kobayashi, S., Sawano, A., Nojima, Y., Shibuya, M., and Maru, Y. (2004) *FASEB J.* **18,** 929–931
14. Yokouchi, M., Kondo, T., Sanjay, A., Houghton, A., Yoshimura, A., Komiya, S., Zhang, H., and Baron, R. (2001) *J. Biol. Chem.* **276,** 35185–35193
15. Andoniou, C. E., Lill, N. L., Thien, C. B., Lupher, M. L., Jr., Ota, S., Bowtell, D. D., Scaife, R. M., Langdon, W. Y., and Band, H. (2000) *Mol. Cell. Biol.* **20,** 851–867
16. Lupher, M. L., Jr., Songyang, Z., Shoelson, S. E., Cantley, L. C., and Band, H. (1997) *J. Biol. Chem.* **272,** 33140–33144
17. Lupher, M. L., Jr., Rao, N., Lill, N. L., Andoniou, C. E., Miyake, S., Clark, E. A., Druker, B., and Band, H. (1998) *J. Biol. Chem.* **273,** 35273–35281
18. Fong, C. W., Leong, H. F., Wong, E. S., Lim, J., Yusoff, P., and Guy, G. R. (2003) *J. Biol. Chem.* **278,** 33456–33464
19. Rubin, C., Litvak, V., Medvedovsky, H., Zwang, Y., Lev, S., and Yarden, Y. (2003) *Curr. Biol.* **13,** 297–307
20. Ohrt, T., Mancini, A., Tamura, T., and Niedenthal, R. (2004) *Cell Signal.* **16,** 1291–1298

21. Liu, J., Kimura, A., Baumann, C. A., and Saltiel, A. R. (2002) *Mol. Cell. Biol.* **22,** 3599–3609
22. Ahmed, Z., and Pillay, T. S. (2001) *Biochem. Soc. Trans.* **29,** 529–534
23. Hu, J., Liu, J., Ghirlando, R., Saltiel, A. R., and Hubbard, S. R. (2003) *Mol. Cell* **12,** 1379–1389
24. Minami, A., Iseki, M., Kishi, K., Wang, M., Ogura, M., Furukawa, N., Hayashi, S., Yamada, M., Obata, T., Takeshita, Y., Nakaya, Y., Bando, Y., Izumi, K., Moodie, S. A., Kajiura, F., Matsumoto, M., Takatsu, K., Takaki, S., and Ebina, Y. (2003) *Diabetes* **52,** 2657–2665
25. Mitra, P., Zheng, X., and Czech, M. P. (2004) *J. Biol. Chem.* **279,** 37431–37435
26. Liu, J., DeYoung, S. M., Hwang, J. B., O'Leary, E. E., and Saltiel, A. R. (2003) *J. Biol. Chem.* **278,** 36754–36762
27. Otwinowski, Z., and Minor, W. (1997) *Methods Enzymol.* **276,** 307–326
28. Navaza, J. (1994) *Acta. Crystallogr. Sect. A.* **50,** 157–163
29. Brünger, A. T., Adams, P. D., Clore, G. M., DeLano, W. L., Gros, P., Grosse-Kunstleve, R. W., Jiang, J. S., Kuszewski, J., Nilges, M., Pannu, N. S., Read, R. J., Rice, L. M., Simonson, T., and Warren, G. L. (1998) *Acta. Crystallogr. Sect. D.* **54,** 905–921
30. Jones, T. A., Zou, J. Y., Cowan, S. W., and Kjeldgaard, M. (1991) *Acta. Crystallogr. Sect. A.* **47,** 110–119
31. Wiseman, T., Williston, S., Brandts, J. F., and Lin, L. N. (1989) *Anal. Biochem.* **179,** 131–137
32. Eck, M. J., Shoelson, S. E., and Harrison, S. C. (1993) *Nature* **362,** 87–91
33. Waksman, G., Shoelson, S. E., Pant, N., Cowburn, D., and Kuriyan, J. (1993) *Cell* **72,** 779–790
34. Betancourt, M. R., and Skolnick, J. (2004) *J. Mol. Biol.* **342,** 635–649
35. Peschard, P., Ishiyama, N., Lin, T., Lipkowitz, S., and Park, M. (2004) *J. Biol. Chem.* **279,** 29565–29571
36. Koradi, R., Billeter, M., and Wüthrich, K. (1996) *J. Mol. Graph.* **14,** 51–55
37. Nicholls, A., Sharp, K. A., and Honig, B. (1991) *Proteins* **11,** 281–296